Reduced graphene oxide-nano zerovalent iron assisted anaerobic digestion of dairy wastewater: A potential strategy for CH_4 enrichment

Article *in* Journal of Environmental Chemical Engineering · May 2023

DOI: 10.1016/j.jece.2023.110035

4 authors, including:

Balasubramanian Paramasivan
National Institute of Technology Rourkela
151 PUBLICATIONS **3,520** CITATIONS

SEE PROFILE

Abanti Sahoo
National Institute of Technology Rourkela
24 PUBLICATIONS **344** CITATIONS

SEE PROFILE

Journal of Environmental Chemical Engineering 11 (2023) 110035

Contents lists available at ScienceDirect

Journal of Environmental Chemical Engineering

journal homepage: www.elsevier.com/locate/jece

Reduced graphene oxide-nano zerovalent iron assisted anaerobic digestion of dairy wastewater: A potential strategy for CH_4 enrichment

Roshini Sasidharan [a,*], Arvind Kumar [a], Balasubramanian Paramasivan [b], Abanti Sahoo [a]

[a] Department of Chemical Engineering, National Institute of Technology Rourkela, 769008, India
[b] Agricultural and Environmental Biotechnology Group, Department of Biotechnology and Medical Engineering, National Institute of Technology Rourkela, 769008, India

ARTICLE INFO

Editor: Yujie Men

Keywords:
Reduced graphene oxide
Interspecies electron transport
Anaerobic digestion
Dairy wastewater treatment
Bioenergy
Conductive additives

ABSTRACT

Efficient waste management and alternatives for waste reduction have been the prime factors in achieving sustainable development goals. Large quantities of waste biomass can be transformed to energy by anaerobic fermentation. This study focused on improving the electron transport and subsequent CH_4 enrichment in the anaerobic digestion of dairy wastewater by adding reduced graphene oxide-nano zerovalent iron (RGO-NZVI) composite. Different ratios (wt/wt) of RGO and NZVI were added to the anaerobic digesters and monitored their effects on biogas volume, composition, COD removal and VFA accumulation. There was 86.27 ± 2.8% high CH_4 and 47.37 ± 1.3% improved COD removal in the digester containing the conductive additive compared to control. Comparing different ratios of RGO-NZVI revealed that a proportion of 2:1 was beneficial for maximum CH_4 generation. Further, it was found that higher concentrations of the conductive additives could be fatal for microbial metabolism. A ratio of 0.5:1 had minimal support on degradation and the composition of CH_4 in this digester was 34.14 ± 1.5% less than control. The metagenomic analysis showed that the diversification of microbial community and switching of major mechanism to direct interspecies electron transfer caused higher CH_4 generation.

1. Introduction

India contributes about 22% towards global milk production, positioning it as the largest milk producer in the world [1]. The quantity of wastewater generated could be as high as ten times the volume of milk processed in the industry [2]. Techniques such as photocatalysis, electro-coagulation, constructed wetlands, precipitation and membrane techniques were applied and studied to treat dairy wastewater [3–6]. These methods need high investment as installation, operation and maintenance are expensive and require a large quantity of chemicals and high energy consumption [6,7]. Dairy waste possesses a high potential to serve as a substrate for microbial metabolism and growth due to its rich composition containing proteins, fats, carbohydrates and other organic stabilizers [8,9]. Inorganic trace nutrients such as potassium, sodium, calcium, magnesium, iron, phosphate, nitrate, nitrite, ammonium, and sulfate are sufficiently available in dairy waste with a favorable pH range [2]. Considering these, dairy waste could be taken as a suitable raw material for anaerobic digestion. While, the improper management of these wastes may lead to uncontrolled evolution of intermediates and degradation products into the environment [10]. Also, anaerobic digestion has been appraised as an attractive method for recovering the bioenergy engrossed in wastes and thus, it helps to reduce the dependency on fossil fuels, creating a circular economy [11].

Biogas is a byproduct of convoluted syntrophic microbial pathways in which the initial phase has been dominated by the non-methanogenic microbes [12]. Since, the performance of an anaerobic system is influenced by the electron transfer interaction, DIET helps to achieve faster microbial kinetics [13,14]. Pretreatment such as acid-based hydrolysis during the ensiling process, incorporation of an electrochemical system, manipulation of operation pressure, improving H_2 to CO_2 ratio and CO_2 enrichment within the digester are examples of digestion enhancement strategies [11,15–18]. Carbon-based conducting additives are gaining attention these days as they buffer the system by resisting reduction in pH, facilitate attached electroactive biofilm formation, act as

Abbreviations: COD, chemical oxygen demand; DIET, direct interspecies electron transfer; EDC, 1-ethyl-3-(3-dimethyl aminopropyl)-carbodiimide; FTIR, fourier transform infrared spectroscopy; NHS, N-hydroxysuccinimide; NZVI, nano-zerovalent iron; RGO, reduced graphene oxide; SCOD, soluble COD; SEM, scanning electron microscopy; VFA, volatile fatty acid; XRD, X-ray Diffraction spectroscopy.

* Corresponding author.
E-mail address: roshinipnkl@gmail.com (R. Sasidharan).

https://doi.org/10.1016/j.jece.2023.110035
Received 31 January 2023; Received in revised form 29 March 2023; Accepted 29 April 2023
Available online 2 May 2023

alternatives of e-pili or cytochrome-c, boost protein degradation and reduce lag time for methanogenesis [13,19,20]. In a study, an anaerobic microbial electrolysis cell has taken advantage of graphene's high surface area and electron mobility to stimulate the species diversification [21]. Similarly, the addition of RGO caused changes in dominant species in the media, increased the production of extracellular polymeric compounds, and improved CH_4 concentration [22]. Even though, more biogas volume was recorded, the total CH_4 content remained unvaried. The applicability of valorization techniques depends on efficiency for CH_4 enrichment. A detailed optimization of operating conditions need to be performed in order to apply such techniques in full-scale.

Researchers also observed remarkable effects in methanogenesis in the presence of metallic and metallic oxide nanoparticles [23]. The changes in metabolism highly depend on the diversity of the microbial population and the chemical form of nanoparticle [24]. Iron-based nanoparticles showed excellent performance as an additive among the nanomaterials studied [25]. In this regard, zerovalent iron (ZVI) is a low-cost, non-toxic and highly reductive substance. In a study, micron-sized ZVI improved the hydrolysis process and regulated the acidification process during the anaerobic treatment of domestic wastewater. Further, ZVI could control pH and ORP and caused a higher propionate conversion rate [26]. Lizama et al. (2019) showed that adding NZVI improved the COD and protein solubilization and aided the formation of highly oxidative radicals (OH·). In anaerobic environments, NZVI is oxidized to ferrous iron, producing hydrogen (Eq. 1) [27,28]. Similarly, NZVI helps to remove free oxygen present in the media, lethal for obligate anaerobes [28].

$$Fe^0 + 2H^+ \rightarrow Fe^{2+} + H_2 \Delta G^0 = -5.02 \frac{KJ}{mol} Fe^0 \quad (1)$$

However, high concentrations of NZVI ($\geq$30 mM) may cause cell disruption and inhibition causing decrease in pH and accumulation of VFA [29]. Further, nanoparticles of iron have a great tendency for aggregate formation due to inter-particle magnetic dipolar interaction, London attractive and van der Walls forces. Some anchoring materials may help to improve the stability of these particles [30,31]. In a study, activated carbon-supported NZVI acted as a combination of multiple tiny micro-batteries for phenol degradation [30]. In a similar study, the inhibition caused by the addition of sharp RGO nanosheets was reduced using magnetite-RGO composite and ensued in superoxide anion-independent oxidation [31]. The application of composites is a way of synergizing the advantages of two or more materials to bring out more beneficial effects than a compound alone. However, previous researches discussed different composites, a comprehensive investigation on the constitution of composites made from RGO and NZVI and their effect on dairy wastewater degradation is lacking.

This article discusses the effects of RGO-NZVI composite in the anaerobic degradation of dairy wastewater to produce CH_4 enriched biogas. The efficiency of the additives was compared by analyzing the wastewater parameters and biogas composition. The mechanistic investigation on effect of the additives was done with the help of metagenomic analysis. Further, the fit of reaction kinetics towards the modified Gompertz model was also evaluated.

2. Materials and methods

2.1. Chemicals and substrates

All the chemicals used in this study were of analytical grade. RGO was purchased from Techinstro (India) and used after removing any impurities by acid treatment [32]. The organic coated NZVI (Nanofer 25DS) was purchased from Nanoiron, Czech Republic and stored at 4 °C in an oxygen-free environment to retain stability. EDC and NHS were purchased from Sigma Aldrich and used without further purification. Glucose, urea, NH_4Cl, $Na_2HPO_4 0.2\ H_2O$, KH_2PO_4, $MgSO_4 \cdot 7\ H_2O$, $FeSO_4 0.7\ H_2O$, $MnSO_4 \cdot H_2O$, $CaCl_2 \cdot H_2O$, $NaHCO_3$, HCl and NaOH were obtained from Himedia (India). Milk powder (Amul, India) and edible yeast were purchased locally. Fresh cow dung was obtained from a local cattle farm (Odisha, India).

2.2. Sludge and synthetic wastewater

Synthetic dairy wastewater was prepared by dissolving the milk powder and nutrients as per the composition given in the supplementary document (Table S1). The C/N ratio of the media was adjusted using glucose. The methanogenic seed inoculum composed of anaerobically enriched cow dung was prepared according to Dong et al. (2019). Initial properties of the dairy wastewater, cow dung, methanogenic seed and feed slurry were determined according to the standard procedures (APHA 2000a) and the results are shown in Table 1 [33].

2.3. Anaerobic batch experiments

The anaerobic digestion was carried out in 1.25 L borosil glass bottles with 1 L working volume and remaining head space. Tedlar gas sampling bags of 1 L capacity were used to collect the biogas formed. Initially, all the batch digesters were fed with 750 mL of dairy wastewater, 200 mL of fresh cow dung and 50 mL of seed to get a final SCOD of 35010 mg L^{-1} and C/N ratio of 19.2. The properties of the components in the feed are as given in Table 1. The pH of the mixed slurry was adjusted to 7.5 with 1 M NaOH. Table 2 gives the details of RGO-NZVI composite added in each reactor. The method for synthesis of RGO-NZVI composite by EDC-NHS crosslinking is provided in S1. All the digesters were incubated in triplicates, including the control digester with no additives. Each batch reactor loaded with feed was flushed with N_2 gas for 15 min to flush out the oxygen in the liquid and incubated at 37 °C. The digesters were shaken every 12 hr with slow rotations to mix the contents. Liquid and gas samples were collected from the digesters daily for the first two weeks and twice a week later on. The statistical significance of each set of values was determined by analyses of variance (ANOVA). All the analytical procedures and details of kinetics study are explained in **S1**.

2.4. Microbial community analysis

Shotgun metagenomic analysis was conducted for the mixed liquor solids collected at the end of digestion, to distinguish the active microbial community between control and digester containing RGO-NZVI composite,. The samples were centrifuged at 10,000 rpm and the DNA isolation was carried out with the CTAB based protocol. DNA quality was confirmed by agarose gel electrophoresis. The sequencing was carried out using Illumina Novaseq6000 and the library was prepared by

Table 1
The properties of each component added to the digester.

Properties	DW	Enriched seed sludge	Cowdung	Slurry
SCOD (mg L^{-1})	27,500	65,900	51,300	35,010
BOD/SCOD	0.38	0.35	0.21	0.38
Total nitrogen (mg L^{-1})	850	1200	0.44[a]	810
C/N ratio	16.82	19.96	21.75	19.2
pH	6.65	5.89	6.13	6.82
Total Solids (g L^{-1})	21.93	84.18	17.94[a]	58.63
Total Volatile Solids (g L^{-1})	19.73	65.11	77.81 * *	47.36
Total Fixed Solids (g L^{-1})	2.20	19.05	22.19 * *	11.26
Total Suspended Solids (g L^{-1})	4.05	49.070	61.40 * *	10.53
Total Dissolved Solids (g L^{-1})	17.88	35.11	38.60 * *	48.10
Cellulose (x10^{-3} g L^{-1})	-	5.08	10.18[a]	18.29
Protein (g L^{-1})	5.83	8.26	4.75	7.86

[a] wt% (g/g); * *% of TS

Table 2
RGO-NZVI composition in each reactor.

Reactor	Dosage (mg L^{-1})	Ratio of RGO-NZVI
R1	900	0.5:1
R2	900	1:1
R3	900	2:1
R4	900	5:1
Control	0	-

Kappa kit (Roche) with 2 * 150 base pair sequencing chemistry. The similarity check was conducted with the help of Reference Sequence (RefSeq) (NR database). Kyoto Encyclopedia of Genes and Genomes (KEGG) database was kept as reference for the prediction of gene functions.

3. Results and discussion

3.1. Effects of RGO-NZVI composite on biogas and CH_4 production

A batch cycle of 36 days duration was conducted with the RGO-NZVI composite containing different ratios of RGO and NZVI. Fig. 1 represents the effect of RGO-NZVI composite addition on biogas and CH_4 production. R2, R3 and R4 gained better mineralization than the control reactor. All the reactors produced a substantial volume of biogas (425–920 mL) on day one and the reactor having an RGO-NZVI ratio of 2:1 (R3) yielded the highest volume of gas (Fig. 1a). On the other hand, the concentration of CH_4 was minimal during the initial stage due to the lag in the bacterial acclimatization when introduced into a new growth environment having high organic loading (Fig. 1c). The different curves in Fig. 1d implied that the control reactor containing no additives had less potential for CH_4 production than R2, R3 and R4. The p-value of 0.005 from the paired t-test analysis indicated a significant difference in the CH_4 production between R3 and control. On the contrary, R1 containing an RGO-NZVI ratio of 0.5:1 produced 34.14 ± 1.5% less CH_4 than the control reactor. The performance of R3 (3841.8 ± 145 mL CH_4) at the end of the digestion was remarkable when compared to R1, R2, R4 and the control reactor with a total CH_4 yield of 1358.15 ± 49 mL, 2892.5 ± 95 mL, 2802.8 ± 105 mL and 2062.4 ± 73 mL of CH_4 respectively (Fig. S1). From the observations, it was clear that active methanogenesis occurred from day 5–14 after an initial lag phase, contributing to more than 75% of total CH_4 production in each of the digesters. Eventually, after this period, the biodegradation entered an idle phase with minimal CH_4 and biogas production (Fig. 1b). Throughout anaerobic digestion, the highest daily production of CH_4 in each of the reactors were 221.4 ± 7.1 mL on day 6, 320.1 ± 4.4 on day 7, 429 ± 18.1 mL, 343.75 ± 7.5 mL and 290 ± 6.38 mL on day 6 from R1, R2, R3, R4 and control reactor respectively. Highly enriched biogas was found in R3 with a CH_4 content of 70 ± 2.8% on day 7, while the control reactor contained only 52 ± 1.5% CH_4 on the same day. Meanwhile, the concentration of CH_4 from R1, R2 and R4 were 48 ± 1.9%, 66 ± 0.9% and 59 ± 1.7%, respectively, on day 7. 34.79 ± 1.3% of the total biogas generated in R3 (11,040 ± 452.64 mL) was constituted by CH_4. Though the CH_4 composition of total biogas from control was 41.58 ± 1.4%, the total volume of biogas at the end of the digestion period was 55.1 ± 2.1% less than that from R3. Considering the specific CH_4 production with respect to COD, R3 could yield 150.6 ± 7.2 mL per g of COD removed, dominating the performance of other reactors R1, R2, R4 and control reactor by 85.84 ± 3.9%, 14.07 ± 0.6%, 12.35 ± 0.6% and 26.4 ± 1.1% respectively. A paired t-test of all the results obtained from R2 and R4 showed a very less significant difference ($p > 0.05$) between the performances, implying similar biochemical behavior of the digestion system [34].

The better CH_4 production in R3 could be attributed to the synchronized effect of iron supplement for microbial growth and DIET supported by electrically active RGO-NZVI composite. The composite facilitates the formation of short passages for electron movements and this assists in the intensified reduction of CO_2 by hydrogen and proliferation of methanogens [35,36]. Moreover, the planar structure of RGO

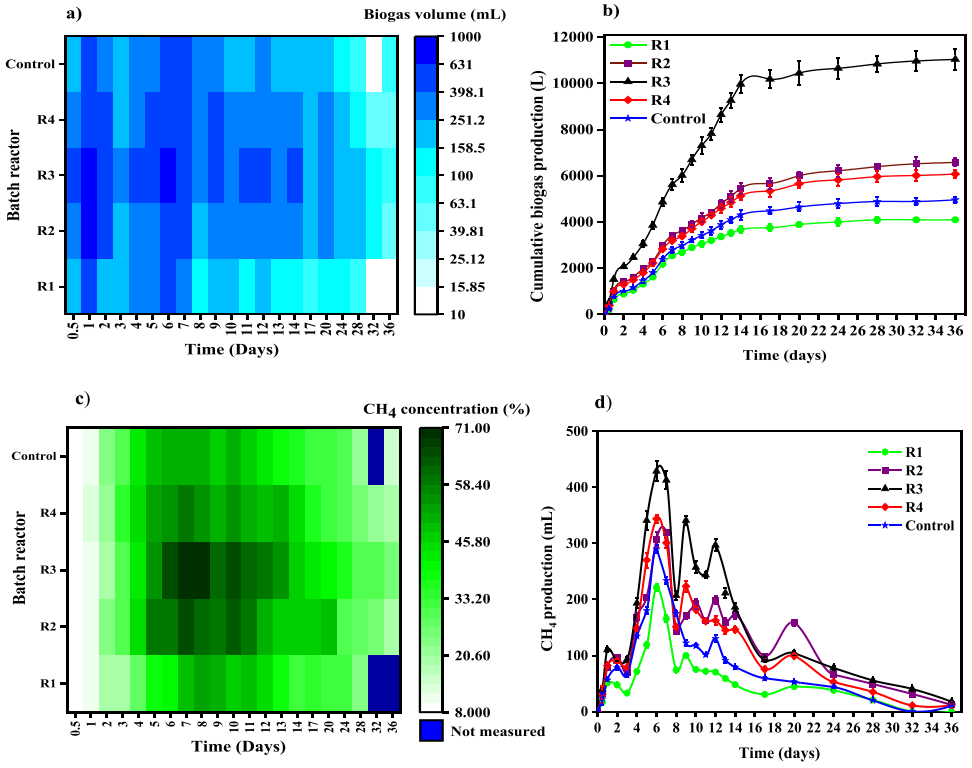

Fig. 1. The volume of biogas on each sampling (a), cumulative volume of biogas (b), composition (c) and volume (d) of CH_4 produced from each batch reactor during the digestion.

provides a high specific surface area for the attached growth of anaerobic bacteria [19]. Further, the distribution of the nanocomposite in the bulk media coordinates the optimum utilization of organic matter by the attached microbes, rather than localized depletion of nutrients as by the settled biomass sludge [37]. However, NZVI at high concentration may cause disruption of cell structure and low consumption of intermediate metabolic products [38,39]. In this study, R1 with higher NZVI (equivalent to ~400 mg L^{-1}) tended to produce less volume of CH_4 and showed a low rate of CH_4 enrichment compared to control. This is a clear indication of toxicity imparted by iron [40]. Meanwhile, lower NZVI concentration in R2 (~300 mg L^{-1}) and R3 (~200 mg L^{-1}) benefitted the metabolism and fostered CH_4 concentration. Carbonaceous amendments have been reported to activate the electron-accepting redox moieties and enable efficient IET between these materials and structures such as conductive pili or outer membrane cytochromes [41]. The difference in redox peak current in the cyclic voltammogram shows (Fig. 7b) that the sludge from R3 has better redox properties than that from the control reactor. The presence of external conductive materials improved the abundance of electroactive units, enhancing the electron transport [42]. Nevertheless, a rise of RGO to ~500 mg L^{-1} of effective concentration was unfavorable, showing less product gas compared to the results exhibited by R3. This could be related to the theory of cytotoxicity imparted by carbonaceous materials causing oxidative stress and perturbation on microbial cell membranes, discussed by Lin et al. and Qu et al. [43,44]. Therefore, it is deduced that the dosage of NZVI and RGO influences CH_4 production and enrichment. This conclusion contradicts the results of Covarrubias-García et al., 2020, who demonstrated the potential inhibition by RGO as dose independent. But, the discussion by Lin et al. (2017) and Muratçobanoğlu et al. (2021) supports the dose-dependent toxicity observations of this study. However, it is worth noting that many factors can influence efficiency since toxicity depends on the concentration, the size, chemical and physical structure, the grade of reduction or oxidation, and the type of microorganisms present in the biological system [31]. In general, it has been found that the addition of RGO-NZVI composite can impart negative or positive effects on wastewater degradation and production of CH_4 in anaerobic digestion processes depending on the ratio of RGO to NZVI in the composite. Table S3 shows a comparison between efficiencies of different additives in improving anaerobic digestion.

During the final stage of degradation, as shown in Fig. 1b, most reactors exhibited no significant gas production. The decline of substrates and the intolerable C/N ratio of media could lead the biological system to reach a plateau of degradation [45]. Switching to the nitrogen-consuming pathways and ammonia inhibition might have played a role in reaching the stationary phase [46]. Also, the depletion of other trace nutrients was reported to cause alterations in the ratio of methanogenic species and might contribute to the lower yields of CH_4 [47].

3.2. Reduction of organic load in the feed

The SCOD of slurry during anaerobic digestion starts decreasing when the mineralization of its biodegradable fraction commences [48]. Fig. 2a shows the trend of SCOD (%) in each reactor during digestion. The highest degradation was observed in R3 with 72.86 ± 2.2% removal and the final concentration of SCOD in R3 was 47.94 ± 1.9%, 27.48 ± 1.1%, 32.62 ± 1.3% and 46.32 ± 2.2% less than that of R1, R2, R4 and control, respectively. Anaerobic digestion begins with hydrolytic and acidogenic microorganisms, decomposing complex substrates into products such as simple sugars, proteins and VFAs [49]. The release of these compounds into the media stimulates acetogenic and methanogenic archaea and eventually, the redox reactions between species and substrates bring down the concentration of these intermediate products [50]. Fig. 3a shows the variation of total VFAs in the reactors during digestion. A high concentration of VFA imparted more SCOD than the initial feed; however, initialization of aceto-cum-methanogenesis consumed VFAs for the growth and metabolism, causing a faster reduction of SCOD [51,52]. Apart from consuming VFAs, stabilization of sugars, proteins and fats would also have contributed to the reduction of SCOD [53]. As depicted in Fig. 3a, R3 contained a high VFA of 390.828 ± 10.9 mg L^{-1} on day 10 and got diminished by further digestion. R1 accumulated VFA at a level higher than other digesters after 8 days and reached a final concentration of 751.394 ± 16.1 mg L^{-1}. Acetic acid was the prominent VFA in all the reactors during the active methanogenesis period (Fig. S2). Though the concentration of propionic acid was low on day 3 in R1; there was a rise up, reaching a higher concentration than acetic acid from day 8. The higher concentration indicated the lesser potential for propionic acid oxidation and conversion into low carbon-chain acids in R1 [19]. The slow rate of propionate uptake due to high-level iron inhibition caused this accumulation in the media [40]. Since the VFA concentration progressively increased in R1, it is clear that the NZVI toxicity affected mainly acetogens and methanogens than the microbes involved in hydrolysis and acidogens. The lesser VFA accumulation in R3 than the control reactor implied that the RGO-NZVI composite had influenced the electron transport and faster consumption of these intermediate compounds. Overall, the high SCOD removal was found from R3 due to the nanocomposite supplement and assisted in maximum utilization of organic substrates from the wastewater [54].

Fig. 2b shows the trend of pH over the digestion period. The sudden decline of pH from 7.3 ± 0.1–6.2 ± 0.06 in R3 until day 2 can be related to the accumulation of VFA in the media due to fast hydrolysis and acidogenesis but delayed methanogenesis [55]. Comparing Figs. 1d and 2b, the pH started to improve favorably from the commencement of methanogenesis because of the subsidence of VFA concentration and slow dissolution of iron [31]. The acetoclastic route could be the dominant methanogenic mechanism in the initial period rather than the hydrogenotrophic production, as the media pH appeared to be in the

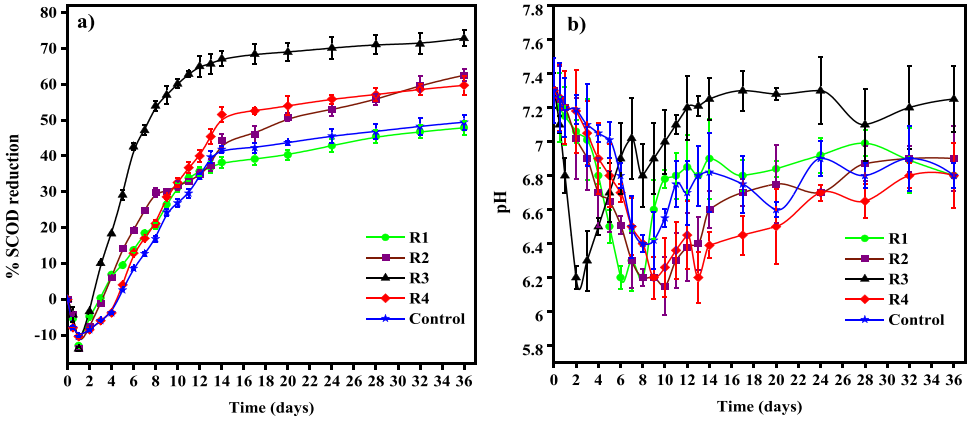

Fig. 2. SCOD reduction (a) and variation of pH (b) in each batch reactor along the duration of digestion.

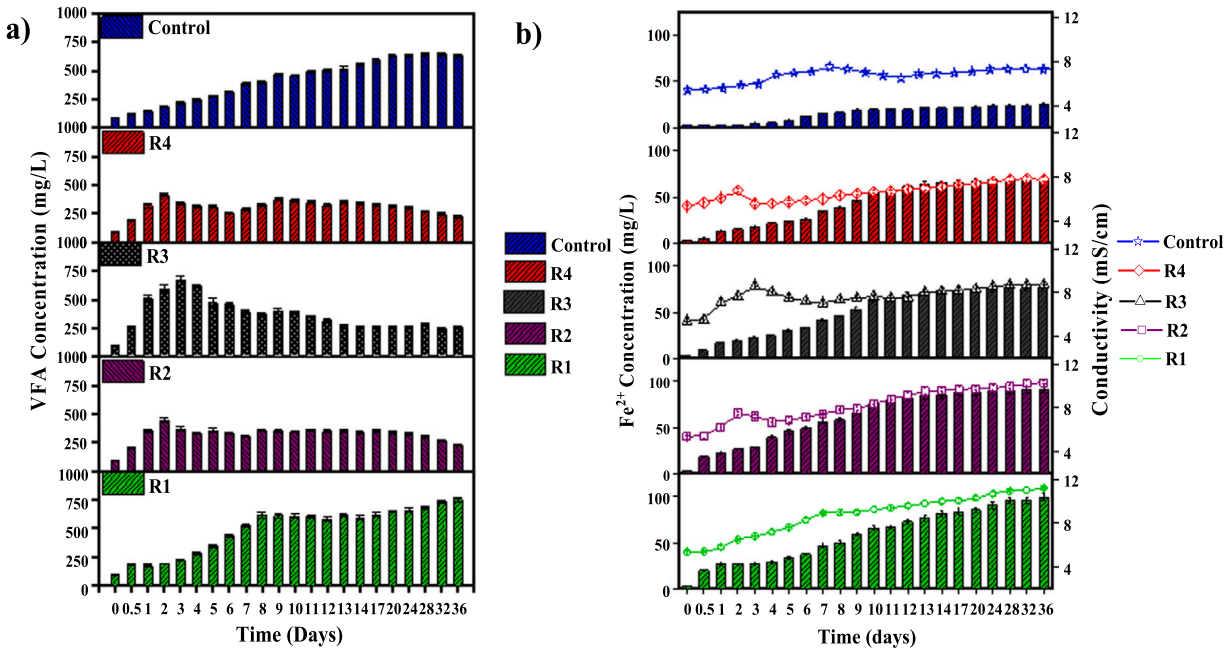

Fig. 3. VFA concentration (a) and Fe^{2+} release and conductivity of the media (b) in digesters throughout the digestion.

acidic range. However, hydrogenotrophic CH_4 production would have prevailed when pH in R3 increased [56]. Likewise, in the anaerobic systems with high NH_3 concentration, methanogenesis shifts from acetoclastic to hydrogenotropic pathway [54,57]. So in this study, the acetoclastic species contributed much toward initial biogas production and eventually shifted to hydrogenotropic methanogenesis. Here, the conductive nanocomposite persuaded methanogenic pathway by supporting electron transport rather than with the mere assistance of hydrogen [19]. However, H^+ as a shuttling medium has not been quantified here. Though VFA accumulation was consistent in R1, high NZVI caused the generation of more hydroxyl ions and thus buffered the reactor from day 6 [31,58]. However, the variation of mixed liquor pH in R2 and R4 was insignificant. This could be attributed to the cumulative effect of the VFAs and the mineralization of nitrogen and phosphorus into nitrites/nitrates and orthophosphates [59]. Overall, the methanogenesis was boosted due to two possible reasons. One is due to the acceleration of initial phase, hydrolysis cum acidogenesis and subsequent CH_4 rise and the second, the methanogenesis itself [60]. But, the evidences of electron shuttle between methanogenic species need to be understood with more precise genetic investigation.

Conductivity is an indirect measure of dissolved ions in a solution. Incubation of anaerobic media with suspended RGO-NZVI composite for a long duration has caused the leaching of iron into the liquid phase. At the end of the batch study, the concentration of Fe^{2+} was found to be proportional to the ratio of iron in the nanocomposite added, as shown in Fig. 3b. The final concentrations were 99.53 ± 4.1, 91.12 ± 3.7, 76.01 ± 2.3, 69.41 ± 2.1 and 25.01 ± 1.2 mg L^{-1} in R1, R2, R3, R4 and control, respectively. The iron released into the control reactor could be due to the mineralization of biomass containing iron, such as plant-based cattle feed in cow dung [61]. The Fe^{2+} concentration in other reactors would be cumulative of leaching from the composite and co-release while mineralization of biomass [59]. Fig. 3b also contains the variation in conductivity measured during the digestion in each of the digesters. Noticeably, the VFA concentration also influenced the ionic density and hence increased the conductivity [62].

3.3. NH_4^+ production during anaerobic digestion

NH_3 is an inhibitory byproduct of anaerobic digestion. NH_4^+ is relatively harmless to the microorganisms in the biogas process and beneficial at concentrations less than 200 mg L^{-1}. The existence of NH_3 in an ionized form is highly pH-dependent. At low pH, more NH_3 will be ionized to form NH_4^+ [37]. Fig. 4 depicts the production of NH_4^+ in the liquid media during microbial activity. In the case of R1, NH_4^+ concentration was less during the initial digestion period and since then, there has been a prominent rate of increase in the ionic form of NH_3. This high concentration of NH_4^+ in R1 gives a glimpse of the inhibition of microbial activity, resulting in less CH_4 production [57]. The reduced concentration of NH_4^+ during the initial startup period might be due to the low mineralization and ammonification of nitrogenous substrates such as amino acids, proteins, uric acid and fat [19]. Further, the rising NH_4^+ probably caused excessive randomness of gene expressions influencing the energy metabolism and signal transduction during microbial digestion in R1 [57,63].

On the other hand, NH_4^+ concentrations in R2, R3 and R4 abruptly increased when pH was reduced, but a rise in pH later on did not reduce the NH_4^+ concentration [37]. The combined effect of degradative evolution and the formation of the NH_3-phosphate complex would have played a role in maintaining the level in R3 [64]. By the end of the digestion, the control reactor contained 1753.81 ± 54.3 mg L^{-1} of NH_4^+. By this, the overall NH_4^+ solubilization in R2, R3 and R4 was 41.2 ± 1.1%, 50.08 ± 2.9% and 42.39 ± 1.6% less than control respectively. NZVI in aqueous media reduces nitrate concentration by forming nitrite and NH_3 [28]. The possibility of degradation of EPS and other cytoplasmic organs in the debris of microbial biomass (due to NZVI inhibition) might have contributed to the high nitrogen content, which are high in proteins and contribute ammonification in R1 [65].

3.4. Effects of RGO-NZVI composite on Microorganisms

The most abundant and representative populations of microbes present in R3 and control digesters are given in Fig. 5. The species-wise classification showed that *Methanosaeta, Methanosarcinales* and *Methanobrevibacter* were the most frequent groups in R3 and the major CH_4 contributor belonging to archaea. The control showed the presence of more hydrogenotrophic methanogens, *Methanobrevibacter, Methanoculleus* and *Methanocorpusculum.* The relative abundance of *Methanosaeta* and *Methanosarcinales* demonstrates the possibility of their participation in DIET for CH_4 production in R3 rather than being produced from the hydrogenotrophic pathway. The high volume of CH_4

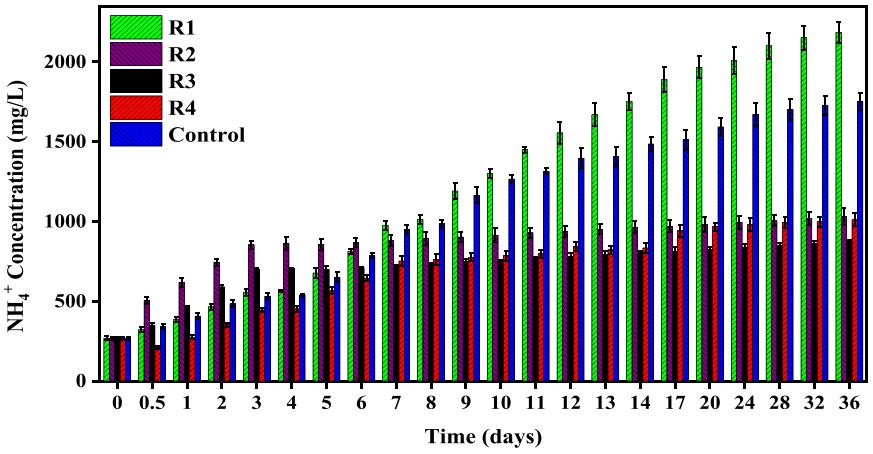

Fig. 4. NH_4^+ accumulation during the digestion.

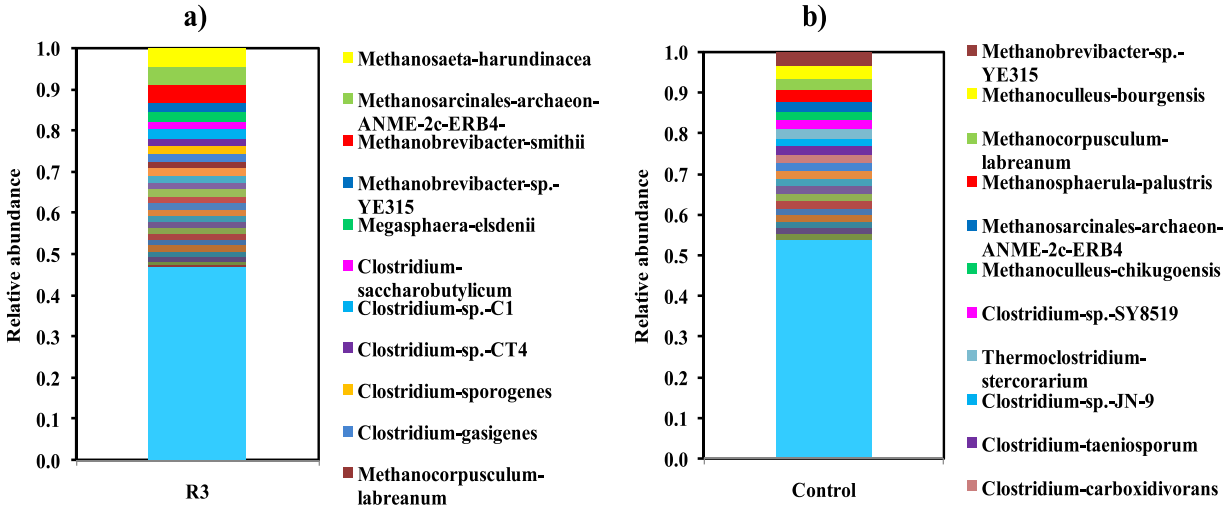

Fig. 5. Relative abundance of main archaeal and bacterial species in R3 (a) and control digesters (b).

produced from R3 is relatable to this phenomenon with heavy-duty methanogens such as *Methanosaeta* and *Methanosarcinales.* The enrichment of hydrogen consumer, *Methanobrevibacter* in R3 could be attributed to the amendment of NZVI and it is in agreement with the previous reports [66,67]. It is reported that certain species belonging to *Methanobacter* could also participate in DIET, which are usually considered as hydrogenotrophs [68]. So the species such as *Methanobrevibacter millerae* would have also contributed to CH_4 via DIET. There are also reports saying the direct electron uptake from NZVI by microbes instead of depending upon other electron donors. Such a relation exists between Fe corrosion and sufate reducing bacteria, which is environmentally significant [69]. Here, R3 was found to be rich in sulfate and iron-reducing bacteria such as *Desulfovibrio*, *Desulfotomaculum*, *Desulfitobacterium* and *Desulfofundulus*, which are active in DIET also. For example, abundant *Desulfotomaculum-ferrireducens* participate in DIET with the high gene expression for *c*-type cytochromes [70,71]. However, certain cytochromes that are not essential are down-regulated to less abundance in DIET systems [72]. The existence of interspecies electron channel by attracting the conductive composite is confirmed by the expression of iron complex receptor protein, as shown in Fig. 6a. The dominance in the expression of peptide binding protein in R3 shows that the amyloid protein on the cell surface binds to the RGO-NZVI composite with the binding protein and facilitates the direct electron transfer for *Methanosaeta* [73]. The presence of ferrous ion transport protein indicates the active role of iron in microbial activities. These complexes are directed towards the inner membrane electron carriers. In addition to the assistance in methanogenesis, ferrous ions could also have engaged in gene regulation and nucleic acid synthesis [74]. The role of homologous genes for Fe^{2+} reduction and periplasmic transport proteins may need to be examined further in this study [60]. The frequency of genes for the expression of pyruvate-ferredoxin oxidoreductase (PFOR), a chief enzyme in anaerobic metabolism, was highest in R3. The formation of low potential ferredoxins helps for electron transport and hydrogen evolution and *Desulfovibrio* has been a dynamic organism in ferredoxin activity [75]. Another organism, *Magnetospirillum,* appeared in R3, hints about the alteration of microbial population upon adding iron [76]. It is essential to quantify the existence of microbe to microbe and Fe to microbe electron transfer. A much detailed mechanistic investigation based on genetics might be necessary while conducting some gene deletion approach to confirm the effect on DIET. Future study to understand the effect of magnetic field in the proliferation of species in an anaerobic digester supplemented with RGO-NZVI would be necessary.

Fig. 6b and c show the phylum level classification of the microbes identified. The introduction of RGO-NZVI additive to the anaerobic digester resulted in diversification of the microbial population compared to control, with a 63.3% more count of microbial species in R3. The phylum euryarchaeota was the highest in R3, whereas firmicutes dominated in the control digester. The dominance of firmicutes refers to efficient hydrolysis followed by hindered methanogenesis. The rise of VFA's in control could be due to this suppression of methanogens

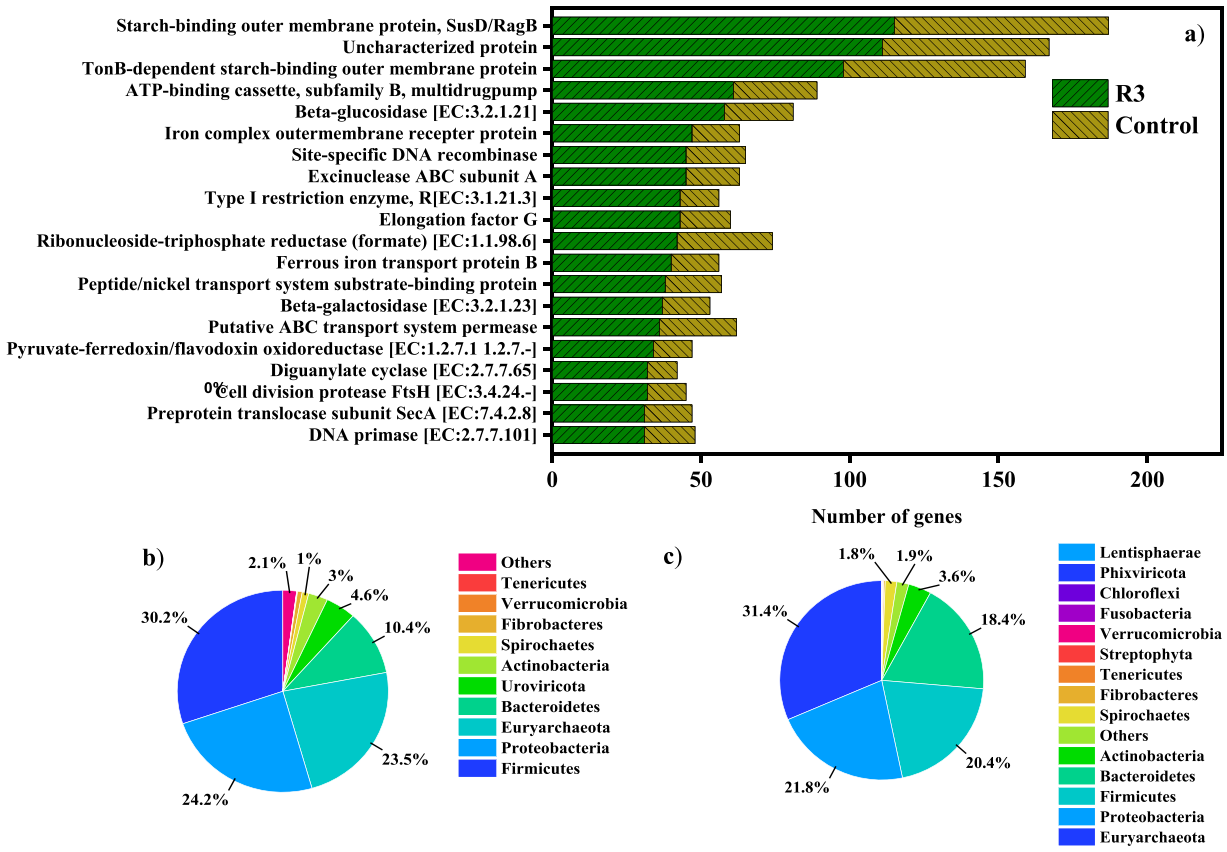

Fig. 6. abundance of genes for major functionalities observed (a), phylum level classification of microbes observed in control digester (b) and R3 (c).

[77]. In total, 234 genera of microbes were identified in R3 and 156 in control. *Clostridium* followed by *Acidaminococcus*, hydrolytic bacteriae, appeared as the significant genera of bacteria in R3 and they accounted for 16.47% and 3.59%, respectively. Also, the control digester favored *Clostridium* and *Prevotella* as dominant genera with 13.58% and 3.54%, respectively. The abundance of firmicutes was reduced in R3 compared to control, probably due to the spike of iron in the media [78]. Other bacterial species, *Escherichia*, an indicator organism, appeared in both the reactors and the numbers were lesser in R3 compared to control, inferring the inactivation of indicator organisms in the presence of NZVI [79]. However, a report by Kim et al., 2018 says that the presence of *Escherichia* could have assisted in the fermentation of organic pollutants during digestion and produced intermediates for CH_4 generation [80].

These results suggest that the amendment of conductive additives into the digester helped to improve the spatial diversity of microbial species positively affecting organic waste degradation. Furthermore, the DIET was aided and enhanced by adding RGO-NZVI composite into the media.

3.5. Kinetics of biomethane generation

The experimental space of anaerobic digestion of dairy wastewater fitted well to the modified Gompertz equation and the parameters of nonlinear fitting are provided in Table 3. Adding the nanocomposite in an RGO to NZVI ratio of 2:1 gave an enhanced CH_4 production rate up to 86.4 ± 1.6% compared to the control digester. The control showed better production by 52.18 ± 1.8% than R1 due to the possible iron toxicity imparted towards methanogenesis. According to the model, the difference in the lag phase time (λ) calculated for each digester is insignificant. However, the values of λ varied as R3 >R4 >control>R2 >R1, providing no inference regarding the influence of additives on λ. This result contradicts the observations by Abdelsalam et al., 2017, who stated that iron additives reduced the lag phase compared to the control. According to the model, the daily CH_4 yield was highest in R3 with 42.66 ± 1.1% more than control and lowest in R1, 34.47 ± 1.2% less than the control digester. Fig. 7a depicts the nonlinear fitting of experimental and calculated CH_4 production. The near to unity values of R^2 and suitable regression parameters demonstrate that the model can fit well and describe the CH_4 volumes obtained from the experiments. The higher peaks of R3 compared to the control reactor in the cyclic voltammetry curve (Fig. 7b) implied that the conductive molecules may activate the redox reactions among the species and substrate molecules and mediate the electron shuttle [13]. Though higher quantities of the conductive conduits impart better electron transport, biocompatibility is a factor that needs to be considered when applied for microbial co-digestion. Faster redox reactions

Table 3
Modified Gompertz model fitting parameters for digesters supplied with different ratios of the nanocomposite.

Model parameter	$M_{0,exp}$ (mL)	M_0 (mL)	R_{max} (mL/day)	λ (Day)	R^2
R1	1358.15 ± 40.74	1344.35 ± 12.43	137.33 ± 4.37	2.13 ± 0.15	0.996
R2	2892.5 ± 57.85	2873.61 ± 21.46	241.08 ± 5.37	2.15 ± 0.12	0.998
R3	3841.8 ± 188.24	3814.35 ± 28.33	365.51 ± 8.90	2.56 ± 0.12	0.998
R4	2802.8 ± 70.07	2786.35 ± 18.29	264.64 ± 5.66	2.22 ± 0.11	0.998
Control	2062.4 ± 72.25	2045.82 ± 13.43	209.57 ± 4.74	2.18 ± 0.11	0.998

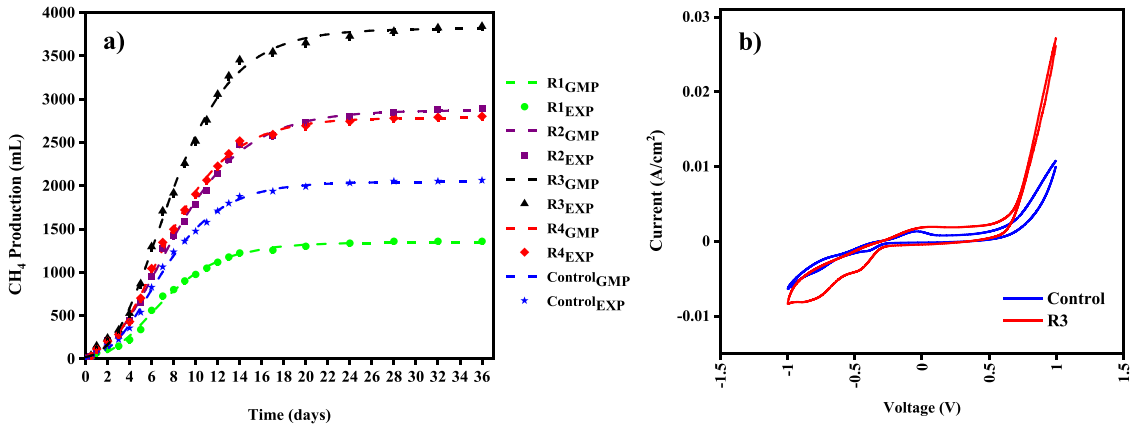

Fig. 7. Nonlinear curve fit of experimental data (EXP) to modified Gompertz model (GMP) for all the digesters studied (a) and electrochemical behavior of sludge material by cyclic voltammetry (b).

with less trouble of toxicity and improved electron shuttle exhibited in R3 makes it as a better anaerobic digestion environment. In this study, the optimum ratio of RGO and NZVI was concluded to be 2:1.

DW contains large quantities of fats and proteins, nitrogen-rich substrates. At higher temperatures, dissolution of organic nitrogen increases; thus, the release rate of nitrogen might be unfavorable for maintaining the C/N ratio to get optimum performance. High temperature may increase the chances of deionizing ammonium to form NH_3, which is harmful and toxic [13]. So, mesophilic digestion is desirable in the case of DW degradation. Also, DW as a substrate holds the potential to enrich the digestate with nitrogen released from proteins and fats and produce a nutritious biofertilizer [81].

3.6. Structural properties and characteristics of RGO-NZVI composite

Fig. S3 represents the XRD and FTIR patterns for the RGO-NZVI composite. The XRD analysis of the composite showed multiple peaks representing RGO and two ionic forms of iron, i.e., zerovalent and trivalent. The sharp peak appeared at 45.21° and less intense peaks at 65.28° and 82.51° show the presence of NZVI in the composite and confirmed with the pattern produced by [82]. Whereas the signals obtained at 30.73°, 35.32°, 55.03° and 71.54° are an illustration of tri and divalent iron molecule, formed sparingly on the surface of NZVI due to oxidation [83]. Thus the composition of NZVI could be explained as a core structure with Fe^0 and a shell structure made of oxides of iron, which is formed via the oxidation of Fe^0 in the core by water and oxygen during the synthesis process [28]. A wide curvature and a peak point at 20.19° were consistent with the previously reported patterns of RGO [31].

The as-synthesized RGO-NZVI nanocomposite was characterized by FTIR spectroscopy and it is shown in Fig. S3b here the spectra contained characteristic peaks for both RGO and NZVI. The bands at 679, 825 and 1059 cm^{-1} represent characteristic Fe-O bond, Fe–O–H bending vibration of FeOOH particle [83] present probably from the oxidized outer surface of NZVI while exposure to the air and alkoxy (C-O) stretching vibrations in the oxidized domains of RGO and due to H_2O respectively [83,84]. The peaks at 2152 and 2983 cm^{-1} could indicate the alkynes in the unoxidized carbons in the RGO and alkane stretch, respectively [85,86]. The minor peaks at 3118, 3610 and 3622 cm^{-1} could be due to the free alcohol stretching and vibrations that remained due to ethanol washing [87]. The peaks at 1540 cm^{-1}, 1695 cm^{-1} and a minor peak at 2270 cm^{-1} support the presence of primary and secondary amine, amide functional group and isocyanates due to crosslinking aided by EDC-NHS [88,89].

The morphology analysis of the RGO-NZVI composite showed a precise formation of NZVI onto the surface of RGO. The surface of RGO was decorated with small aggregates of NZVI by amino functionality, imparted by EDC-NHS crosslinking [83]. Intrinsic agglomeration could be prevented by affixing NZVI in this way [90]. In Fig. 8a, the NZVI incorporated on the layers of RGO is encircled, which confirms the crosslinking. EDX analysis also indicated similar results showing an iron content of 17.08%. The morphological variation of spent composite as shown in Fig. 8b clearly indicates the active participation of RGO-NZVI composite in anaerobic digestion. Further, the surface is characterized by biofilm formation during anaerobic digestion. This attached growth of bacteria possibly reduced the interspecies distance and facilitated DIET resulting in more biogas production [36].

4. Conclusions

In the present study, a demonstration of enhanced CH_4 production from DW by adding RGO-NZVI composite was conducted. The results implied that the conductive additives helped improve biogas production and reduce the organic load in the DW by mediating the electron transport between functional microbial species. Here, the attached growth of microbial biomass onto the conductive supplement ensured the optimum utilization of available substrates and sharing of electrons between Fe and cells. The simultaneous digestion in the presence of various ratios of the conductive materials showed that the outcomes of the RGO-NZVI composite addition into anaerobic digestion are dose-dependent and may cause inhibitory effects in the system at higher NZVI dosages. Further, the NH_4^+ concentration played an essential part in the reactor, which exhibited inhibition in low efficiency reactors. The analysis of microbial community revealed that the abundance and diversity of methanogenic species could be altered by the conductive composites added. So, the addition of RGO-NZVI composite is beneficial, when incorporated into an anaerobic system handling high fat waste.

Funding

This research was carried out as a part of a sponsored project by Department of Science and Technology (DST), Government of India (GoI) through Water Technology Initiative [File No. DST/TMD-EWO/WTI/2K19/EWFH/2019/312].

CRediT authorship contribution statement

Roshini Sasidharan: Conceptualization, Design of experiments, Collection and analysis of data, Manuscript preparation. **Arvind Kumar:** Conceptualization, Supervision, Revision, Editing and suggestions. **Balasubramanian Paramasivan:** Conceptualization, Supervision, Revision, Editing and suggestions. **Abanti Sahoo**: Conceptualization, Supervision, Revision and suggestions.

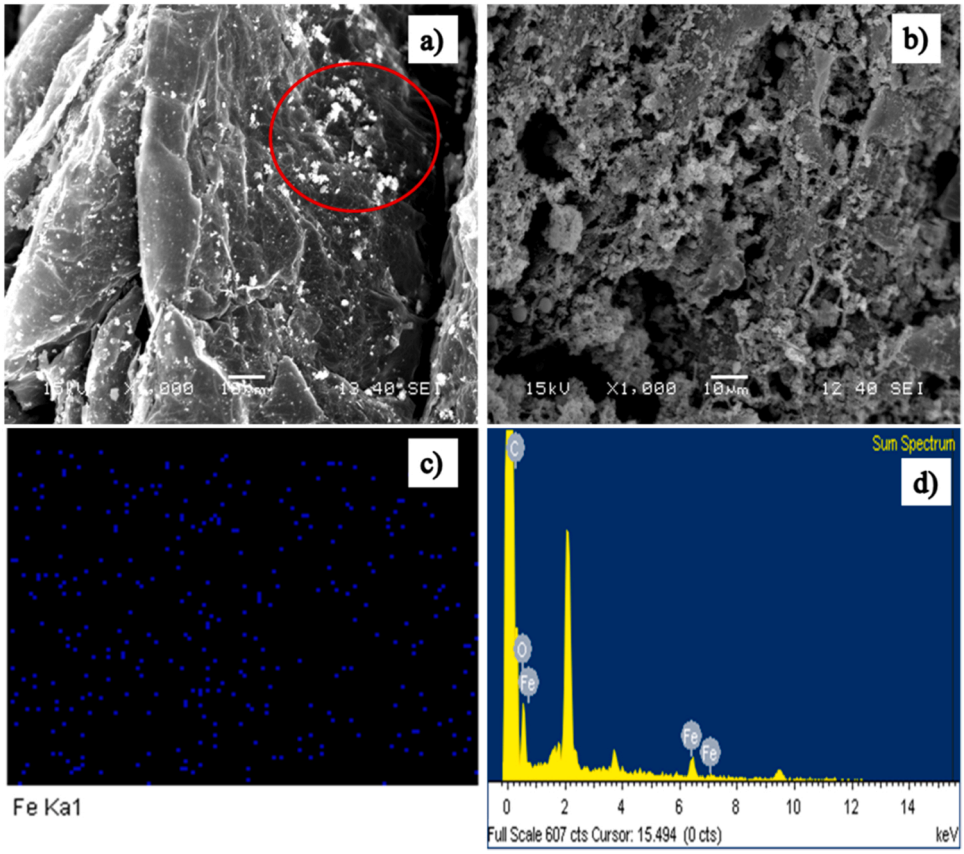

Fig. 8. SEM images of RGO-NZVI before adding to the digester (a) and attached growth on the surface of the conductive composite after 36 days of digestion (b). EDX mapping of iron on RGO-NZVI composite (c) and EDX spectrum of the RGO-NZVI composite.

Declaration of Competing Interest

The authors declare that they have no known competing financial interests or personal relationships that could have appeared to influence the work reported in this paper.

Data availability

No data was used for the research described in the article.

Acknowledgment

The authors are thankful to the National Institute of Technology Rourkela for providing the necessary research facilities and technical assistance.

Appendix A. Supporting information

Supplementary data associated with this article can be found in the online version at doi:10.1016/j.jece.2023.110035.

References

[1] FAOSTAT, Food and Agriculture Organization of the United Nations, 2021. https://www.fao.org/faostat/en/#data/QCL.
[2] R.J. Marassi, L.G. Queiroz, D.C.V.R. Silva, F.T. da Silva, G.C. Silva, T.C.B. d Paiva, Performance and toxicity assessment of an up-flow tubular microbial fuel cell during long-term operation with high-strength dairy wastewater, J. Clean. Prod. 259 (2020), https://doi.org/10.1016/j.jclepro.2020.120882.
[3] M.A. Barakat, M. Anjum, R. Kumar, Z.O. Alafif, M. Oves, M.O. Ansari, Design of ternary Ni(OH)2/graphene oxide/TiO2 nanocomposite for enhanced photocatalytic degradation of organic, microbial contaminants, and aerobic digestion of dairy wastewater, J. Clean. Prod. 258 (2020), 120588, https://doi.org/10.1016/J.JCLEPRO.2020.120588.
[4] B. Chezeau, L. Boudriche, C. Vial, A. Boudjemaa, Treatment of dairy wastewater by electrocoagulation process: Advantages of combined iron/aluminum electrodes, Sep. Sci. Technol. 55 (2020) 2510–2527, https://doi.org/10.1080/01496395.2019.1638935.
[5] M.C. Schierano, M.C. Panigatti, M.A. Maine, C.A. Griffa, R. Boglione, Horizontal subsurface flow constructed wetland for tertiary treatment of dairy wastewater: Removal efficiencies and plant uptake, J. Environ. Manag. 272 (2020), 111094, https://doi.org/10.1016/J.JENVMAN.2020.111094.
[6] T. Yonar, Ö. Sivrioğlu, N. Özengin, Physico-Chemical Treatment of Dairy Industry Wastewaters: A Review, Technol. Approaches Nov. Appl. Dairy, Process (2018), https://doi.org/10.5772/INTECHOPEN.77110.
[7] S.G. and R.T. Piercristiano Brazzale, Brice Bourbon, Pierre Barrucand, Mark Fenelon, Wastewater Treatment In Dairy Processing Innovative Solutions for Sustainable Wastewater Management, Bull. Int. Dairy Fed. 500/2019. (2019).
[8] Z. Usmani, M. Sharma, J. Gaffey, M. Sharma, R.J. Dewhurst, B. Moreau, J. Newbold, W. Clark, V.K. Thakur, V.K. Gupta, Valorization of dairy waste and by-products through microbial bioprocesses, Bioresour. Technol. 346 (2022), 126444, https://doi.org/10.1016/J.BIORTECH.2021.126444.
[9] T.F. Ferreira, P.A. Santos, A.V. Paula, H.F. de Castro, G.S.S. Andrade, Biogas generation by hybrid treatment of dairy wastewater with lipolytic whole cell preparations and anaerobic sludge, Biochem. Eng. J. 169 (2021), 107965, https://doi.org/10.1016/J.BEJ.2021.107965.
[10] J.R. Kim, K.G. Karthikeyan, Effects of severe pretreatment conditions and lignocellulose-derived furan byproducts on anaerobic digestion of dairy manure, Bioresour. Technol. 340 (2021), 125632, https://doi.org/10.1016/J.BIORTECH.2021.125632.
[11] H. Sun, J. Li, X. Cui, W. Stinner, J. Guo, R. Dong, Enhancement mechanism of biogas potential from lignocellulosic substrates in the ensiling process via acid-based hydrolysis and biological degradation, J. Clean. Prod. 319 (2021), 128826, https://doi.org/10.1016/j.jclepro.2021.128826.
[12] S. Ren, M. Usman, D.C.W. Tsang, S. O-Thong, I. Angelidaki, X. Zhu, S. Zhang, G. Luo, Hydrochar-Facilitated Anaerobic Digestion: Evidence for Direct Interspecies Electron Transfer Mediated through Surface Oxygen-Containing Functional Groups, Environ. Sci. Technol. 54 (2020) 5755–5766, https://doi.org/10.1021/acs.est.0c00112.
[13] P. Wang, H. Peng, S. Adhikari, B. Higgins, P. Roy, W. Dai, X. Shi, Enhancement of biogas production from wastewater sludge via anaerobic digestion assisted with biochar amendment, Bioresour. Technol. 309 (2020), 123368, https://doi.org/10.1016/J.BIORTECH.2020.123368.
[14] R. Shekhar Bose, B. Chowdhury, B.S. Zakaria, M. Kumar Tiwari, B. Ranjan Dhar, Significance of different mixing conditions on performance and microbial

communities in anaerobic digester amended with granular and powdered activated carbon, Bioresour. Technol. 341 (2021), 125768, https://doi.org/10.1016/J.BIORTECH.2021.125768.
[15] P. Kumar, V. Kumar, J. Singh, P. Kumar, Electrokinetic assisted anaerobic digestion of spent mushroom substrate supplemented with sugar mill wastewater for enhanced biogas production, Renew. Energy 179 (2021) 418–426, https://doi.org/10.1016/J.RENENE.2021.07.045.
[16] I. Díaz, F. Fdz-Polanco, B. Mutsvene, M. Fdz-Polanco, Effect of operating pressure on direct biomethane production from carbon dioxide and exogenous hydrogen in the anaerobic digestion of sewage sludge, Appl. Energy 280 (2020), 115915, https://doi.org/10.1016/J.APENERGY.2020.115915.
[17] V. Corbellini, C. Feng, M. Bellucci, A. Catenacci, T. Stella, A. Espinoza-Tofalos, F. Malpei, Performance analysis and microbial community evolution of in situ biological biogas upgrading with increasing H2/CO_2 ratio, Archaea (2021)) (2021), https://doi.org/10.1155/2021/8894455.
[18] M. Muntau, M. Lebuhn, D. Polag, Y. Bajón-Fernández, K. Koch, Effects of CO_2 enrichment on the anaerobic digestion of sewage sludge in continuously operated fermenters, Bioresour. Technol. 332 (2021), 125147, https://doi.org/10.1016/j.biortech.2021.125147.
[19] D. Johnravindar, B. Liang, R. Fu, G. Luo, H. Meruvu, S. Yang, B. Yuan, Q. Fei, Supplementing granular activated carbon for enhanced methane production in anaerobic co-digestion of post-consumer substrates, Biomass-.-. Bioenergy 136 (2020), 105543, https://doi.org/10.1016/J.BIOMBIOE.2020.105543.
[20] G. Wang, J. Zhu, Y. Xing, Y. Yin, Y. Li, Q. Li, R. Chen, When dewatered swine manure-derived biochar meets swine wastewater in anaerobic digestion: A win-win scenario towards highly efficient energy recovery and antibiotic resistance genes attenuation for swine manure management, Sci. Total Environ. 803 (2022), https://doi.org/10.1016/j.scitotenv.2021.150126.
[21] Y. Liu, Y. Li, R. Gan, H. Jia, X. Yong, Y.C. Yong, X. Wu, P. Wei, J. Zhou, Enhanced biogas production from swine manure anaerobic digestion via in-situ formed graphene in electromethanogenesis system, Chem. Eng. J. 389 (2020), 124510, https://doi.org/10.1016/J.CEJ.2020.124510.
[22] H. Muratçobanoğlu, Ö.B. Gökçek, R.A. Mert, R. Zan, S. Demirel, The impact of reduced graphene oxide (rGO) supplementation on cattle manure anaerobic digestion: Focusing on process performance and microbial syntrophy, Biochem. Eng. J. 173 (2021), 108080, https://doi.org/10.1016/J.BEJ.2021.108080.
[23] G.K. Hassan, A. Abdel-Karim, M.T. Al-Shemy, P. Rojas, J.L. Sanz, S.H. Ismail, G. G. Mohamed, F.A. El-gohary, A. Al-sayed, Harnessing Cu@Fe3O4 core shell nanostructure for biogas production from sewage sludge: Experimental study and microbial community shift, Renew. Energy 188 (2022) 1059–1071, https://doi.org/10.1016/J.RENENE.2022.02.087.
[24] G. Amo-Duodu, S. Rathilal, M.N. Chollom, E. Kweinor Tetteh, Application of metallic nanoparticles for biogas enhancement using the biomethane potential test, Sci. Afr. 12 (2021), e00728, https://doi.org/10.1016/J.SCIAF.2021.E00728.
[25] M. Yazdani, M. Ebrahimi-Nik, A. Heidari, M.H. Abbaspour-Fard, Improvement of biogas production from slaughterhouse wastewater using biosynthesized iron nanoparticles from water treatment sludge, Renew. Energy 135 (2019) 496–501, https://doi.org/10.1016/J.RENENE.2018.12.019.
[26] Y. Zang, Y. Yang, Y. Hu, H.H. Ngo, X.C. Wang, Y.Y. Li, Zero-valent iron enhanced anaerobic digestion of pre-concentrated domestic wastewater for bioenergy recovery: Characteristics and mechanisms, Bioresour. Technol. 310 (2020), 123441, https://doi.org/10.1016/j.biortech.2020.123441.
[27] A.C. Lizama, C.C. Figueiras, L.A. Gaviria, A.Z. Pedreguera, J.E.Ruiz Espinoza, Nanoferrosonication: A novel strategy for intensifying the methanogenic process in sewage sludge, Bioresour. Technol. 276 (2019) 318–324, https://doi.org/10.1016/j.biortech.2019.01.021.
[28] J. Kodikara, B. Gunawardana, M. Jayaweera, M. Sudasinghe, J. Manatunge, Nitrate removal in potable groundwater by nano zerovalent iron under oxic conditions, Water Pract. Technol. 15 (2020) 1126–1143, https://doi.org/10.2166/wpt.2020.086.
[29] Y. Yang, J. Guo, Z. Hu, Impact of nano zero valent iron (NZVI) on methanogenic activity and population dynamics in anaerobic digestion, Water Res 47 (2013) 6790–6800, https://doi.org/10.1016/J.WATRES.2013.09.012.
[30] D. Dong, R. Wang, P. Geng, C. Li, Z. Zhao, Enhancing effects of activated carbon supported nano zero-valent iron on anaerobic digestion of phenol-containing organic wastewater, J. Environ. Manag. 244 (2019) 1–12, https://doi.org/10.1016/j.jenvman.2019.04.062.
[31] I. Covarrubias-García, G. Quijano, A. Aizpuru, J.L. Sánchez-García, J.L. Rodríguez-López, S. Arriaga, Reduced graphene oxide decorated with magnetite nanoparticles enhance biomethane enrichment, J. Hazard. Mater. 397 (2020), 122760, https://doi.org/10.1016/J.JHAZMAT.2020.122760.
[32] R. Ikram, B.M. Jan, W. Ahmad, Advances in synthesis of graphene derivatives using industrial wastes precursors; prospects and challenges, J. Mater. Res. Technol. 9 (2020) 15924–15951, https://doi.org/10.1016/J.JMRT.2020.11.043.
[33] APHA, Standard Methods for the Evaluation of Water and Wastewater. 18th Edition, American Public Health Association, Washington DC, 2000.
[34] J.L. Linville, Y. Shen, R.P. Schoene, M. Nguyen, M. Urgun-Demirtas, S.W. Snyder, Impact of trace element additives on anaerobic digestion of sewage sludge with in-situ carbon dioxide sequestration, Process Biochem 51 (2016) 1283–1289, https://doi.org/10.1016/j.procbio.2016.06.003.
[35] P. Jadhav, M. Nasrullah, A.W. Zularisam, P. Bhuyar, S. Krishnan, P. Mishra, Direct interspecies electron transfer performance through nanoparticles (NPs) for biogas production in the anaerobic digestion process, Int. J. Environ. Sci. Technol. (2021) 1–13, https://doi.org/10.1007/S13762-021-03664-W.
[36] M. Harb, Y. Xiong, J. Guest, G. Amy, P.Y. Hong, Differences in microbial communities and performance between suspended and attached growth anaerobic membrane bioreactors treating synthetic municipal wastewater, Environ. Sci. Water Res. Technol. 1 (2015) 800–813, https://doi.org/10.1039/C5EW00162E.
[37] P. Biplob, S. Fatihah, Z. Shahrom, E. Ahmed, Nitrogen-removal efficiency in an upflow partially packed biological aerated filter (BAF) without backwashing process, J. Water Reuse Desalin. 1 (2011) 27–35, https://doi.org/10.2166/WRD.2011.008.
[38] J. Cheng, J. Hua, T. Kang, B. Meng, L. Yue, H. Dong, H. Li, J. Zhou, Nanoscale zero-valent iron improved lactic acid degradation to produce methane through anaerobic digestion, Bioresour. Technol. 317 (2020), 124013, https://doi.org/10.1016/J.BIORTECH.2020.124013.
[39] Y. Pan, P.Y. Leung, Y.Y. Li, J. Chen, R.Y.C. Kong, N.F.Y. Tam, Enhancement effect of nanoscale zero-valent iron addition on microbial degradation of BDE-209 in contaminated mangrove sediment, Sci. Total Environ. 781 (2021), 146702, https://doi.org/10.1016/J.SCITOTENV.2021.146702.
[40] E. Kwietniewska, J. Tys, Process characteristics, inhibition factors and methane yields of anaerobic digestion process, with particular focus on microalgal biomass fermentation, Renew. Sustain. Energy Rev. 34 (2014) 491–500, https://doi.org/10.1016/J.RSER.2014.03.041.
[41] C. Luo, F. Lü, L. Shao, P. He, Application of eco-compatible biochar in anaerobic digestion to relieve acid stress and promote the selective colonization of functional microbes, Water Res 68 (2015) 710–718, https://doi.org/10.1016/J.WATRES.2014.10.052.
[42] G. Ren, P. Chen, J. Yu, J. Liu, J. Ye, S. Zhou, Recyclable magnetite-enhanced electromethanogenesis for biomethane production from wastewater, Water Res 166 (2019), 115095, https://doi.org/10.1016/j.watres.2019.115095.
[43] Y. Qu, Q. Ma, J. Deng, W. Shen, X. Zhang, Z. He, J.D.V. Nostrand, J. Zhou, J. Zhou, Responses of microbial communities to single-walled carbon nanotubes in phenol wastewater treatment systems, Environ. Sci. Technol. 49 (2015) 4627–4635, https://doi.org/10.1021/ES5053045/SUPPL_FILE/ES5053045_SI_001.PDF.
[44] R. Lin, J. Cheng, J. Zhang, J. Zhou, K. Cen, J.D. Murphy, Boosting biomethane yield and production rate with graphene: The potential of direct interspecies electron transfer in anaerobic digestion, Bioresour. Technol. 239 (2017) 345–352, https://doi.org/10.1016/J.BIORTECH.2017.05.017.
[45] A. Cerón-Vivas, K.T. Cáceres, A. Rincón, Á.A. Cajigas, A. Cerón-Vivas, K.T. Cáceres, A. Rincón, Á.A. Cajigas, Influence of pH and the C/N ratio on the biogas production of wastewater, Rev. Fac. Ing. Univ. Antioquia (2019) 70–79, https://doi.org/10.17533/UDEA.REDIN.20190627.
[46] X. Wang, X. Lu, F. Li, G. Yang, Effects of Temperature and Carbon-Nitrogen (C/N) Ratio on the Performance of Anaerobic Co-Digestion of Dairy Manure, Chicken Manure and Rice Straw: Focusing on Ammonia Inhibition, PLoS One 9 (2014), https://doi.org/10.1371/JOURNAL.PONE.0097265.
[47] B. Wintsche, K. Glaser, H. Sträuber, F. Centler, J. Liebetrau, H. Harms, S. Kleinsteuber, Trace elements induce predominance among methanogenic activity in anaerobic digestion, Front. Microbiol. 7 (2016) 2034, https://doi.org/10.3389/FMICB.2016.02034/BIBTEX.
[48] C. Bougrier, A. Battimelli, J.P. Delgenes, H. Carrere, Combined Ozone Pretreatment and Anaerobic Digestion for the Reduction of Biological Sludge Production in Wastewater Treatment, Ozone Sci. Eng. 29 (2007) 201–206, https://doi.org/10.1080/01919510701296754.
[49] H. Liu, Y. Chen, Enhanced Methane Production from Food Waste Using Cysteine to Increase Biotransformation of l -Monosaccharide, Volatile Fatty Acids, and Biohydrogen, Environ. Sci. Technol. 52 (2018) 3777–3785, https://doi.org/10.1021/ACS.EST.7B05355/SUPPL_FILE/ES7B05355_SI_001.PDF.
[50] Z. Zhao, Y. Li, X. Quan, Y. Zhang, Towards engineering application: Potential mechanism for enhancing anaerobic digestion of complex organic waste with different types of conductive materials, Water Res 115 (2017) 266–277, https://doi.org/10.1016/J.WATRES.2017.02.067.
[51] C. Li, P. Champagne, B.C. Anderson, Enhanced biogas production from anaerobic co-digestion of municipal wastewater treatment sludge and fat, oil and grease (FOG) by a modified two-stage thermophilic digester system with selected thermo-chemical pre-treatment, Renew. Energy 83 (2015) 474–482, https://doi.org/10.1016/J.RENENE.2015.04.055.
[52] A.N. Nozhevnikova, Y.I. Russkova, Y.V. Litti, S.N. Parshina, E.A. Zhuravleva, A. A. Nikitina, Syntrophy and Interspecies Electron Transfer in Methanogenic Microbial Communities, Microbiology 89 (2020) 129–147, https://doi.org/10.1134/S0026261720020101/TABLES/2.
[53] O.P. Sahu, P.K. Chaudhari, Removal of color and chemical oxygen demand from sugar industry wastewater using thermolysis processes, N. Pub Balaban 56 (2014) 1758–1767, https://doi.org/10.1080/19443994.2014.956797.
[54] Z. Guo, M. Usman, S.A. Alsareii, F.A. Harraz, M.S. Al-Assiri, M. Jalalah, X. Li, E. S. Salama, Synergistic ammonia and fatty acids inhibition of microbial communities during slaughterhouse waste digestion for biogas production, Bioresour. Technol. 337 (2021), 125383, https://doi.org/10.1016/J.BIORTECH.2021.125383.
[55] K. Khatami, M. Atasoy, M. Ludtke, C. Baresel, Ö. Eyice, Z. Cetecioglu, Bioconversion of food waste to volatile fatty acids: Impact of microbial community, pH and retention time, Chemosphere 275 (2021), 129981, https://doi.org/10.1016/J.CHEMOSPHERE.2021.129981.
[56] R.M. Wormald, S.P. Rout, W. Mayes, H. Gomes, P.N. Humphreys, Hydrogenotrophic Methanogenesis Under Alkaline Conditions, Front. Microbiol. 11 (2020), https://doi.org/10.3389/FMICB.2020.614227/FULL.
[57] N. Zhang, H. Peng, Y. Li, W. Yang, Y. Zou, H. Duan, Ammonia determines transcriptional profile of microorganisms in anaerobic digestion, Braz. J. Microbiol. 49 (2018) 770–776, https://doi.org/10.1016/J.BJM.2018.04.008.
[58] E.L. Tilston, C.D. Collins, G.R. Mitchell, J. Princivalle, L.J. Shaw, Nanoscale zerovalent iron alters soil bacterial community structure and inhibits

chloroaromatic biodegradation potential in Aroclor 1242-contaminated soil, Environ. Pollut. 173 (2013) 38–46, https://doi.org/10.1016/J.ENVPOL.2012.09.018.
[59] A. Yadav, R. Gupta, V.K. Garg, Organic manure production from cow dung and biogas plant slurry by vermicomposting under field conditions, Int. J. Recycl. Org. Waste Agric. 2 (2013) 1–7, https://doi.org/10.1186/2251-7715-2-21/TABLES/5.
[60] D.R. Lovley, Electrotrophy: Other microbial species, iron, and electrodes as electron donors for microbial respirations, Bioresour. Technol. 345 (2022), 126553, https://doi.org/10.1016/J.BIORTECH.2021.126553.
[61] P.S. Erickson, K.F. Kalscheur, Nutrition and feeding of dairy cattle, Anim. Agric. (2020), https://doi.org/10.1016/B978-0-12-817052-6.00009-4.
[62] C.A. Aceves-Lara, E. Latrille, T. Conte, J.P. Steyer, Online estimation of VFA, alkalinity and bicarbonate concentrations by electrical conductivity measurement during anaerobic fermentation, Water Sci. Technol. 65 (2012) 1281–1289, https://doi.org/10.2166/wst.2012.703.
[63] N. Zhang, H. Peng, Y. Li, W. Yang, Y. Zou, H. Duan, Ammonia determines transcriptional profile of microorganisms in anaerobic digestion, Braz. J. Microbiol. 49 (2018) 770–776, https://doi.org/10.1016/j.bjm.2018.04.008.
[64] L. Chen, Y. Gu, C. Cao, J. Zhang, J.W. Ng, C. Tang, Performance of a submerged anaerobic membrane bioreactor with forward osmosis membrane for low-strength wastewater treatment, Water Res 50 (2014) 114–123, https://doi.org/10.1016/J.WATRES.2013.12.009.
[65] N. Romillac, Ammonification, Encycl. Ecol. (2019) 256–263, https://doi.org/10.1016/B978-0-12-409548-9.10889-9.
[66] C.M. Dykstra, S.G. Pavlostathis, Zero-valent iron enhances biocathodic carbon dioxide reduction to methane, Environ. Sci. Technol. 51 (2017) 12956–12964, https://doi.org/10.1021/ACS.EST.7B02777/ASSET/IMAGES/LARGE/ES-2017-02777Y_0003.JPEG.
[67] J. González, M.E. Sánchez, X. Gómez, Enhancing anaerobic digestion: the effect of carbon conductive materials, J. Carbon Res 4 (2018) 59, https://doi.org/10.3390/C4040059.
[68] S. Zheng, F. Liu, B. Wang, Y. Zhang, D.R. Lovley, Methanobacterium capable of direct interspecies electron transfer, Environ. Sci. Technol. 54 (2020) 15347–15354, https://doi.org/10.1021/ACS.EST.0C05525/ASSET/IMAGES/LARGE/ES0C05525_0007.JPEG.
[69] T.L. Woodard, T. Ueki, D.R. Lovley, H_2 is a major intermediate in desulfovibrio vulgaris corrosion of iron, MBio (2023), https://doi.org/10.1128/MBIO.00076-23.
[70] G. Yang, J. Guo, L. Zhuang, Y. Yuan, S.G. Zhou, Desulfotomaculum ferrireducens sp. nov., a moderately thermophilic sulfate-reducing and dissimilatory Fe(III)-reducing bacterium isolated from compost, Int. J. Syst. Evol. Microbiol 66 (2016) 3022–3028, https://doi.org/10.1099/IJSEM.0.001139.
[71] Y. Li, L. Liang, C. Sun, Z. Wang, Q. Yu, Z. Zhao, Y. Zhang, Glycol/glycerol-fed electrically conductive aggregates suggest a mechanism of stimulating direct interspecies electron transfer in methanogenic digesters, Water Res 217 (2022), 118448, https://doi.org/10.1016/J.WATRES.2022.118448.
[72] C. Van Steendam, I. Smets, S. Skerlos, L. Raskin, Improving anaerobic digestion via direct interspecies electron transfer requires development of suitable characterization methods, Curr. Opin. Biotechnol. 57 (2019) 183–190, https://doi.org/10.1016/J.COPBIO.2019.03.018.
[73] K. Gao, Y. Lu, Putative extracellular electron transfer in Methanogenic Archaea, Front. Microbiol. 12 (2021) 649, https://doi.org/10.3389/FMICB.2021.611739/BIBTEX.
[74] S.C. Andrews, A.K. Robinson, F. Rodríguez-Quiñones, Bacterial iron homeostasis, FEMS Microbiol. Rev. 27 (2003) 215–237, https://doi.org/10.1016/S0168-6445(03)00055-X.
[75] E.C. Hatchikian, M. Bruschi, Characterization of a new type of ferredoxin from Desulfovibrio africanus, Biochim. Biophys. Acta - Bioenerg. 634 (1981) 41–51, https://doi.org/10.1016/0005-2728(81)90126-2.
[76] C. Berny, R. Le Fèvre, F. Guyot, K. Blondeau, C. Guizonne, E. Rousseau, N. Bayan, E. Alphandéry, A Method for Producing Highly Pure Magnetosomes in Large Quantity for Medical Applications Using Magnetospirillum gryphiswaldense MSR-1 Magnetotactic Bacteria Amplified in Minimal Growth Media, Front. Bioeng. Biotechnol. 8 (2020) 16, https://doi.org/10.3389/FBIOE.2020.00016/BIBTEX.
[77] M. Chen, S. Liu, X. Yuan, Q.X. Li, F. Wang, F. Xin, B. Wen, Methane production and characteristics of the microbial community in the co-digestion of potato pulp waste and dairy manure amended with biochar, Renew. Energy 163 (2021) 357–367, https://doi.org/10.1016/J.RENENE.2020.09.006.
[78] K. Ma, Z. Cao, Y. Cui, T. Chen, S. Shan, Y. Shi, W. Wang, J. Lv, Effect of magnetite on anaerobic digestion treating saline wastewater: Methane production, biomass aggregation and microbial community dynamics, Bioresour. Technol. 341 (2021), 125783, https://doi.org/10.1016/J.BIORTECH.2021.125783.
[79] M. Mosaferi, R. Zarei, M.H.S. Barhagi, M.A. Jafar-abadi, A. Khataee, Bactericidal effect of starch-stabilized zero-valent iron nanoparticles on *Escherichia coli*, Int. J. Environ. Health Eng. 5 (2016) 2, https://doi.org/10.4103/2277-9183.179195.
[80] N.Y. Kim, S.N. Kim, O. Bin Kim, Long-term adaptation of Escherichia coli to methanogenic co-culture enhanced succinate production from crude glycerol, J. Ind. Microbiol. Biotechnol. 45 (2018) 71, https://doi.org/10.1007/S10295-017-1994-0.
[81] S. Isaksson, Biogas production at high ammonia levels The importance of temperature and trace element supplementation on microbial communities, UPPSALA UNIVERITET. (2018). http://www.teknat.uu.se/student (accessed February 24, 2022).
[82] C. Wu, J. Tu, W. Liu, J. Zhang, S. Chu, G. Lu, Z. Lin, Z. Dang, The double influence mechanism of pH on arsenic removal by nano zero valent iron: electrostatic interactions and the corrosion of Fe0, Environ. Sci. Nano 4 (2017) 1544–1552, https://doi.org/10.1039/C7EN00240H.
[83] N. Mehrabi, A. Masud, M. Afolabi, J. Hwang, G.A. Calderon Ortiz, N. Aich, Magnetic graphene oxide-nano zero valent iron (GO-nZVI) nanohybrids synthesized using biocompatible cross-linkers for methylene blue removal, RSC Adv. 9 (2019) 963–973, https://doi.org/10.1039/C8RA08386J.
[84] M. Fan, T. Li, J. Hu, R. Cao, X. Wei, X. Shi, W. Ruan, Artificial neural network modeling and genetic algorithm optimization for cadmium removal from aqueous solutions by reduced graphene oxide-supported nanoscale zero-valent iron (nZVI/rGO) composites, Mater. 10 (2017) 544, https://doi.org/10.3390/MA10050544.
[85] D. Karimipourfard, R. Eslamloueyan, N. Mehranbod, Novel heterogeneous degradation of mature landfill leachate using persulfate and magnetic CuFe2O4/RGO nanocatalyst, Process Saf. Environ. Prot. 131 (2019) 212–222, https://doi.org/10.1016/J.PSEP.2019.09.009.
[86] Surabhi, D. Sah, J. Shabir, P. Gupta, S. Mozumdar, Imidazole-functionalized porous graphene oxide nanosheets loaded with palladium nanoparticles for the oxidative amidation of aldehydes, ACS Appl. Nano Mater. 5 (2022) 5776–5792, https://doi.org/10.1021/ACSANM.2C00859.
[87] C.H. Lin, Y.C. Chen, P.I. Huang, Preparation of multifunctional dopamine-coated zerovalent iron/reduced graphene oxide for targeted phototheragnosis in breast cancer, Nanomater. 10 (2020) 1957, https://doi.org/10.3390/NANO10101957.
[88] R. Liu, J. Ming, H. Zhang, B. Zuo, EDC/NHS crosslinked electrospun regenerated tussah silk fibroin nanofiber mats, Fibers Polym. 2012 135 13 (2012) 613–617, https://doi.org/10.1007/S12221-012-0613-Y.
[89] J. Hua, Z. Li, W. Xia, N. Yang, J. Gong, J. Zhang, C. Qiao, Preparation and properties of EDC/NHS mediated crosslinking poly (gamma-glutamic acid)/epsilon-polylysine hydrogels, Mater. Sci. Eng. C. 61 (2016) 879–892, https://doi.org/10.1016/J.MSEC.2016.01.001.
[90] T. Bao, M.M. Damtie, A. Hosseinzadeh, R.L. Frost, Z.M. Yu, J. Jin, K. Wu, Catalytic degradation of P-chlorophenol by muscovite-supported nano zero valent iron composite: Synthesis, characterization, and mechanism studies, Appl. Clay Sci. 195 (2020), 105735, https://doi.org/10.1016/J.CLAY.2020.105735.